Research Article

SOHAG JOURNAL OF SCIENCES

https://doi.org/10.21608/sjsci.2024.336812.1233

Antimicrobial Activities of Biogenic Silver Nanoparticles Synthesized by *Curvularia spicifera*

Bahig A. El deeb, Gerges G. Faheem*, Mahmoud S. Bakhit

Department of Botany and Microbiology, Faculty of Science, Sohag University, Sohag, 82524, Egypt.
**E-mail: gem_gad@yahoo.com*

Received: 16th November 2024, **Revised:** 2nd December 2024, **Accepted:** 19th December 2024
Published online: 7th February 2025

Abstract: *Curvularia spicifera* (SUMCC 22003) is an endophytic fungus isolated from leaves of the medicinal plant *Calotropis procera* that were collected from Wadi Bir-EL-Ain, Sohag, Egypt. The fungus was identified based on morphology and phylogenetic analyses. The ability of *C. spicifera* to biosynthesize silver nanoparticles (AgNPs) was studied. The biosynthesized AgNPs were characterized using UV-vis spectroscopy, XRD measurement, DLS, Zeta potential analysis, FTIR and HR-TEM analysis. The formed AgNPs were stable, well-dispersed and spherical crystalline with an average diameter of 38.41 nm and a Zeta potential of -6.35 mV. The FTIR analysis confirmed that AgNPs are capped with protein. The biosynthesis optimization study indicated that 1 mM AgNO3, 5 g of biomass weight, pH 10.5 and a reaction temperature of 60°C were the optimal conditions for AgNPs biosynthesis. AgNPs exerted significant antimicrobial activity at different concentrations against the tested species of Gram-negative bacteria, Gram-positive bacteria and yeast species, demonstrating their potential as broad-spectrum antimicrobial agents. *Escherichia coli* showed the highest susceptibility to AgNPs (50 µg) with an inhibition zone diameter of 23.7±0.3 mm and MIC 4.2±0.1 µg. AgNPs (50 µg) exhibited an inhibition zone of 16.7±0.1 mm and MIC of 5.7±0.3 for *Candida albicans*.
Keywords: *Calotropis procera*, extracellular biosynthesis, characterization, optimization, antimicrobial activity

1. Introduction

Metal nanoparticles can be synthesized by various chemical and physical methods, including solvo-thermal synthesis, laser ablation, chemical reduction, ion sputtering and the sol-gel method [1, 2]. However, these approaches are often expensive, time-consuming, energy-intensive and environmentally harmful [3-5]. In contrast, biological methods are gaining attraction due to their cost-effectiveness, environmentally friendly approach and use of non-toxic chemicals for synthesis [6-8]. Many microorganisms and plant extracts have the capability to produce nanoparticles through biological pathways [9-11]. Fungal-mediated synthesis of nanoparticles is a promising approach in Nano-Biotechnology [12-14]. Compared to bacteria and plants, fungi offer advantages in terms of ease of culture and maintenance in laboratory settings. They secrete substantial amounts of enzymes and proteins, enhancing productivity, ensuring protein coating and promoting high stability while preventing nanoparticle agglomeration [15, 16].

Endophytic fungi are microorganisms that colonize living plant tissue without causing immediate harm or symptomatic infection to their host [17]. They colonize various parts of their plant host, including the root, stem, leaf, flower, fruit and seed [18]. Extracellular biosynthesis of AgNPs by endophytic fungi could streamline downstream processing compared to intracellular biosynthesis [19, 20]. To enhance the yield of biosynthesized AgNPs, it is essential to optimize cultural conditions and various physical parameters such as pH and temperature [21, 22]. Alterations in culture medium composition, pH, temperature, growth time and agitation can impact the metabolism of microorganisms, thereby influencing the physicochemical characteristics of the nanoparticles and the composition of the capping [23].

The use of silver nanoparticles (AgNPs) has been documented since ancient times for a variety of applications, they have been employed in the development of therapeutic agents, disease diagnosis, biosensors and agriculture [24-26]. They are widely utilized for their antimicrobial, anticoagulant and anticancer properties, as well as in medical devices and drug delivery. This is due to its catalytic activity, chemical stability, optical and thermal properties [27]. Silver nanoparticles have shown promise in biomedical applications such as infection prevention and wound healing. Studies have demonstrated their strong antimicrobial activity against various types of bacteria [28-30].

Calotropis procera (Aiton) W. T. Aiton is a desert plant commonly found in tropical and subtropical regions of Africa and Asia [31]. This plant is well-known for its medicinal properties, with various parts exhibiting anti-inflammatory, antioxidant, anticancer and antimicrobial activities [32]. The medicinal properties of the plant can be attributed to their endophytic fungi [33].

Curvularia species are found in subtropical to tropical regions, although a few can also be found in temperate zones [34]. *Curvularia spicifera* (Bainier) Boedijn is globally distributed, isolated from soil and air and has a diverse host range of plants [35]. This study aims to explore the ability of the endophytic fungus *C. spicifera* (SUMCC 22003) to biosynthesize AgNPs. Charchterization, optimization and antimicrobial activities of AgNPs were studied.

2. Materials and methods

2.1. Sample collection and fungal isolation

Curvularia spicifera was isolated from the leaves of the medicinal plant *Calotropis procera* that were collected from Wadi Bir-EL-Ain in eastern desert of Sohag Governorate, Egypt. Isolation of the endophytic fungus followed the method outlined by Hallmann et al. [36]. Isolation and purification were carried out on potato dextrose agar (PDA; Oxoid, Basingstoke, England) and malt extract agar medium (MEA; 2% w/v). Morphological characteristics were observed and photographed in freshwater using using an Olympus BX51 compound microscope (Olympus, Tokyo, Japan) equipped with a digital camera (Toup Tek XCAM1080PHA Toup Tek, Zhejiang, China). The fungus was grown on Czapek yeast extract agar (CYA), MEA, oatmeal agar (OA), PDA and incubated at 25 °C for 7 days. These media allow a comprehensive assessment of the isolate's morphological and physiological characteristics, where each medium has a distinct composition, influencing fungal growth, sporulation and colony morphology. The fungal culture is deposited in Sohag University microbial culture collection, Egypt (SUMCC 22003).

2.2. DNA extraction, sequencing and phylogenetic analyses

Fungal mycelium was obtained from pure fungal cultures grown in glucose and yeast with peptone (GPY) broth [37] and genomic DNA was extracted using the Microbial DNA Extraction Kit (MOBIO; Mo Bio Laboratories, Carlsbad, CA, USA) following the manufacturer's instructions. PCR amplification and sequencing of the ITS regions were conducted using the primer pairs ITS1 and ITS4 [38], following the methods described by Abdel-Wahab et al. [39] by Solgent Co. Ltd (South Korea). Sequencher 4.2.2 (Gene Codes Corporation) was used to assemble the sequences and ClustalX [40] was used to align them with pertinent ones that were obtained from GenBank. Maximum Likelihood (ML), Maximum Parsimony (MP) and Bayesian inference (BI) were used in phylogenetic studies. Maximum likelihood (ML) analysis was carried out under the GTR+GAMMA substitution model with 1000 rapid bootstrap replicates using RAxMLGUI v. 2.0.8101 [41]. Phylogenetic analyses were performed based on details outlined by Abdel-Aziz and Bakhit [42]. The revealed sequence was deposited in NCBI GenBank to obtain the isolate's unique accession number.

2.3. Extracellular biosynthesis of AgNPs by *C. spicifera*

The fungus was cultivated in 100 ml of malt glucose yeast peptone (MGYP) broth in a 250 ml Erlenmeyer flask [43]. The inoculated flasks were incubated at 28°C for 96 hrs. The resulting biomass was harvested and washed with sterilized deionized water after that approximately 10 g (wet weight) of the biomass was transferred to a 250 ml Erlenmeyer flask containing 100 ml of sterilized deionized water. This flask was then subjected to 72 hrs of incubation at 28°C [2]. The biomass was removed and the filtrate was obtained by passing it through Whatman filter paper No.1. The filtrate was then reacted with a known quantity of silver nitrate ($AgNO_3$) to reach an overall silver ion concentration of 1 mM [44]. This reaction was carried out in the dark at 28 °C. Fungus filtrate and the $AgNO_3$ solution were used as controls under similar experimental conditions and the color change was observed for up to 72 hrs [45].

2.4. Characterization of the biosynthesized AgNPs

UV–visible spectra were measured by UV–visible Spectrophotometer (JENWAY 7315 spectrophotometer, UK) in the wavelength range of 300–700 nm to ensure the presence of specific surface Plasmon resonance (SPR) peak of AgNPs.

The crystalline metallic pattern of AgNPs powder was analyzed in a 2θ region from 30° to 80° using (D8 Advance, Germany) X-ray diffractometer operating at 40 mA and 40 kV with Cu Kα radiation (λ=1.54060 Å).

The size distribution of the biosynthesized AgNPs (determined by dynamic light scattering (DLS) technique) and Zeta potential were measured by Malvern Instrument Zetasizer Nano ZS (Malvern, UK).

FTIR spectra of AgNPs and fungal filtrate were recorded in the range of 4000–400/cm^{-1} using FTIR spectroscopy (Platinum-ATR, Bruker Alpha, Germany) to detect the possible biomolecules responsible for reduction, capping and effective stabilization of the biosynthesized AgNPs.

Transmission electron microscopy (TEM) and selected area electron diffraction (SAED) analyses were performed for the biosynthesized AgNPs using the JEOL JSM 100CX TEM instrument, Japan (TEM, Electron Microscope Unit, Cairo University, Egypt). The images of the appeared nanoparticles were captured.

2.4. Optimization of AgNPs biosynthesis

AgNPs were produced under various physiochemical conditions to determine the optimal conditions for producing stable and uniform AgNPs. Optimization of AgNPs biosynthesis involved examining the following factors: $AgNO_3$ concentration, biomass concentration, pH value and the reaction temperature [43, 45, 46]. Each factor was tested by varying only a single parameter at a time. Different $AgNO_3$ concentrations (0.1, 0.5, 1, 2, 3, 4 and 5 mM), biomass weights (5, 10, 15 and 20 g), pH (5.5, 6.5, 7.0, 7.5, 8.5, 9.5 and 10.5) and the reaction temperatures (10, 20, 28, 35, 45 and 60 °C) were investigated. The absorbance of the colored solution that resulted from the reaction for each factor was measured by UV-visible spectrophotometer.

2.5. Antimicrobial activity of the biosynthesized AgNPs

The antimicrobial activities of AgNPs were assayed by disc diffusion method as described by Humphries et al. [47]. The synthesized AgNPs were tested against human pathogens: Gram-negative bacteria (*Escherichia coli* and *Pseudomonas aeruginosa*), Gram-positive bacteria (*Bacillus cereus* and *Staphylococcus aureus* (ACCB 136) and 3 pathogenic yeast strains (*Candida albicans* (AUMC 10440)), *Candida tropicalis* (AUMC 10442) and *Galactomyces candidum* (AUMC 10443)). The test was performed using Mueller-Hinton agar (MHA) for bacterial strains and Sabouraud's dextrose agar (SDA) for yeast strains. Four AgNPs concentrations (5, 10, 25 and 50 µg) were loaded on sterile filter paper discs. Fungal filtrate and $AgNO_3$ discs were used as negative controls.

Ampicillin (10 µg) for bacteria and fluconazole (25 µg) for yeast strains were used as positive controls. The plates were incubated at 37°C for 24 hrs and the appeared clear zones were measured in mm. These assays were carried out in triplicates.

The minimum inhibitory concentration (MIC) of AgNPs was determined for the tested microorganisms by broth microdilution method using 96-well microtiter plates as described by Veiga et al. [48]. The concentrations of AgNPs were adjusted from 0.5 to 50 µg in 0.5 µg increments to facilitate the evaluation. The lowest concentration which completely inhibited the growth of microbes was recorded as MIC. From the above assay, a loopful of inoculum was taken from each well showing no visual growth after incubation and spotted onto MHA/SDA plates to validate the MIC assay.

2.6. Statistical analysis

The software XLSTAT version 2023.2.0 [49] was used to statistically analyze the data using one-way analysis of variance (ANOVA). Every experiment was conducted in triplicate, and the data expressed as mean ± standard deviation [26]. Differences at $P<0.05$ were regarded as statistically significant.

3. Results and discussion

3.1. Identification of the isolated fungus

Identification of the isolated fungus; *Curvularia spicifera* (SUMCC 22003) was carried out based on morphology and phylogenetic analyses.

3.1.1. Phylogenetic analysis

The ITS dataset consisted of 35 taxa, of which 33 belong to the genus *Curvularia* and 2 taxa belong to *Bipolaris* were used as outgroup. The maximum parsimony dataset consists of 451 characters that included: 366 constant, 38 variable parsimony uninformative and 47 parsimony-informative characters. The RAxML analysis of the ITS dataset yielded the best scoring tree (Fig. 1) with a final ML optimization likelihood value of -1367.863893. The matrix had 117 distinct patterns with 5.04% undetermined characters or gaps. Estimated base frequencies were found to be A=0.250583, C=0.245350, G=0.223739, T=0.280328; substitution rates, AC=2.524190, AG=1.074583, AT=1.080545, CG=1.079217, CT=4.495694, GT=1.0. Phylogenetic analysis placed our strain (SUMCC 22003) close to other isolates of Curvularia spicifera (CBS 274.52, CBS 125738, CBS 314.64, CBS 246.62, HN43-6-2, DAOM 575355, CCTU 245, FV-11, LB-28, CBS 198.31).

3.1.2 Taxonomy

Curvularia spicifera (Bainier) Boedijn, Bull. Jard. bot. Buitenz, 3 Sér. 13(1): 127 (1933) [50], (Fig. 2).
GenBank accession number – ITS: PQ587293.
Colony diameter after 6 d (mm) at 25°C: CYA 44–48; MEA 55–60; OA 70–80; PDA 43–50.
Colony characters: On CYA, greenish to olive, fluffy, cottony, margin regular round, undulate, rhizoid; reverse dark brown. On MEA, greyish to olive, margin regular round; reverse dark brown. On OA, greyish to dark olive, texture funiculose, fluffy, cottony, margin regular round reverse black. On PDA, greyish to dark olive, fluffy, cottony, margin irregular round; reverse brown.
Micromorphology: On PDA after 6 days of growth at 25°C, vegetative hyphae pale brown, 3.0–5.5 µm in diameter. Conidiophores pale brown or brown, erect or slightly curved, septate, unbranched, verruculose, mainly 30–85×3.5–5.0 µm (x=65.2×4.5 µm, n=25) and extend to 350–450×5.0–5.5 µm. Conidiogenous cells are brown, sub-cylindrical to irregularly shaped, verruculose, 1-multiple cicatrized, 8.4–20.8 µm in length. Conidia straight, sometimes slightly curved broadly elliptical, dark brown, smooth, 2-3 distoseptate mainly 3, germination from apex, 24–30×8–11 µm (x=25.8×9.8 µm, n=40). Chlamydospores were not observed.
Materials examined: Egypt, Sohag Governorate, Wadi Bir-El-Ain (26°38'36.8"N 31°50'13.5"E), from healthy leaves of *Calotropis procera* (Apocynaceae), Feb. 2022, coll. G. G. Faheem, The culture is deposited in Sohag University microbial culture collection, Egypt (SUMCC 22003).
Hosts and distribution: *Curvularia spicifera* (SUMCC 22003) on *Calotropis procera* in Egypt. Examples of previous findings include its presence on *Helianthus annuus* in Iran [51], on soil in Spain [52], on *Capsicum anuum* and *Buchloe dactyloides* in Cyprus [53], on *Trichosanthes dioica* in India [54], on Barley and wheat in Morocco [55], on *Bouteloua gracilis* in USA [34] and on *Foeniculum vulgare* in Turkey [56].

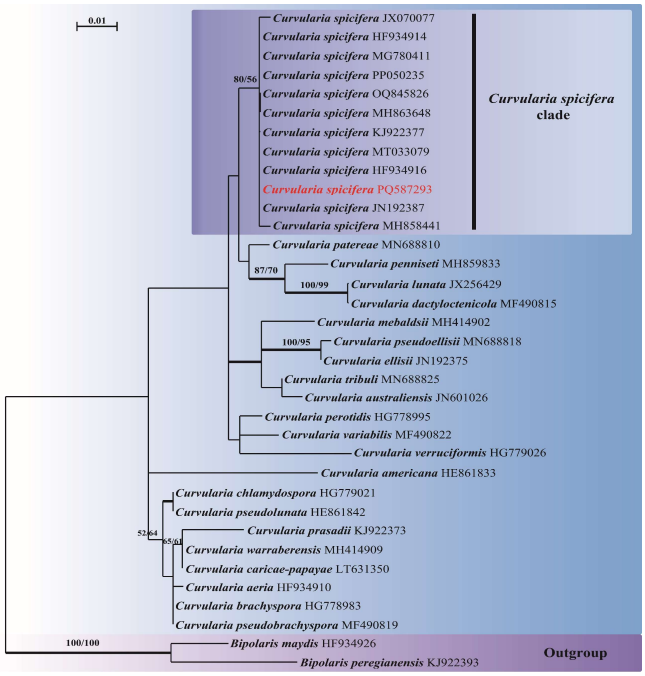

Figure 1. Phylogram generated from ML analysis (RAxML) based on ITS sequence dataset for *Curvularia spicifera* (SUMCC 22003) along with other species of *Curvularia*. Bootstrap support on the nodes represents ML and MP ≥50%. Branches receiving Bayesian PP ≥90% are in bold. The sequence of our new isolate is in red.

3.2. Extracellular biosynthesis and characterization of AgNPs

The color of mycelial free filtrate of *C. spicifera* turned from pale yellow to dark brown after incubation with $AgNO_3$ (1 mM) for 3 days. The color change reflects a primary indication for AgNPs formation [22]. This was further confirmed by UV-visible spectroscopy, which revealed a

distinct surface Plasmon resonance (SPR) peak of AgNPs at 420 nm (Fig. 3A), consistent with the typical range of 400–500 nm [57]. No color changes or significant shifts in the UV-visible spectra were observed for the control samples.

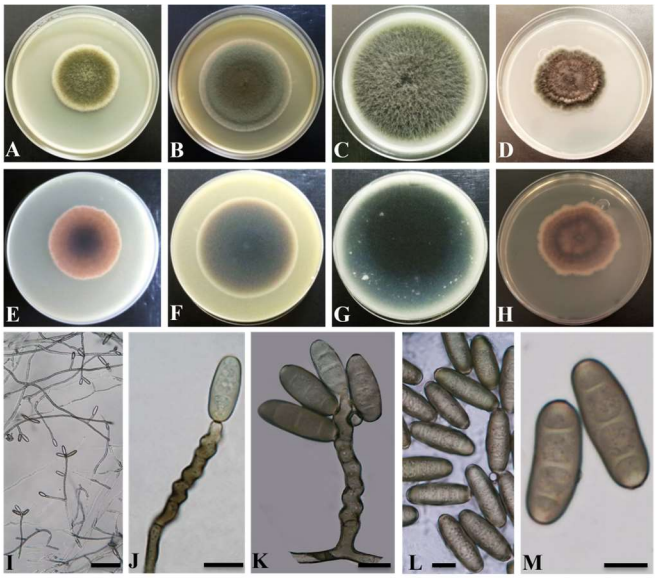

Figure 2. *Curvularia spicifera* (SUMCC 22003). **A**, **B**, **C**, **D.** Colonies on CYA, MEA, OA, and PDA, respectively. **E**, **F**, **G**, **H.** Colonies reverse for the same media, respectively. **I**-**K** Conidiophores and conidiogenous cells. **L**, **M**. Conidia. Scale bars: **I** = 30 µm. **J**-**M** = 10 µm.

The biosynthesized AgNPs exhibited a crystalline structure, as confirmed by XRD analysis. Examination of the XRD pattern (Fig. 3B) demonstrated the presence of a face-centered cubic (FCC) lattice of silver, with diffraction peaks observed at 38.185°, 44.381°, 64.573° and 77.557° corresponding to the (111), (200), (220) and (311) planes, respectively (Pattern: COD 9011607).

DLS analysis of AgNPs demonstruted that the nanoparticles were displayed size range of 27 to 53 nm, with an average diameter of 38.41 nm (Fig. 3C). It is obvious that the most significant factors affecting the size of AgNPs were $AgNO_3$ (mM) followed by reaction pH and filtrate to $AgNO_3$ ratio [58]. The zeta potential of the AgNPs was found to be -6.35 mV (Fig. 3D). These zeta potential values indicate that the colloids demonstrate good stability, likely attributed to the presence of fungal proteins serving as a capping agent with a strongly negative charge on the surface of the AgNPs. This leads to repulsive forces between the particles and prevent agglomeration [59].

FTIR spectra of the synthesized AgNPs and fungal filtrate are shown in (Fig. 3E). They exhibited common peaks, as the stretching of –NH and –OH at 3200 to 3400 cm^{-1}. Characteristic peaks were observed of AgNPs, indicating the formation of new bonds that were absent in the fungal filtrate. For example, peaks at 2920 and 2852 cm^{-1} represented C–H stretching of alkanes [60]. Peaks at 2395 and 2359 cm^{-1} corresponded to $–NH_2$, while the peak at 1587 cm^{-1} was assigned to amide I and amide II. The bands at 1388, 1109 and 618 cm^{-1} were associated with methylene tails of the protein (CH3-R), C-N of aliphatic amines of polyphenols and O-H stretching [58]. The protein capped the nanoparticles by binding to either the free amine groups or cysteine residues [46]. FTIR results indicated that AgNPs were capped with fungal biomolecules that were protein in nature and they were responsible for the synthesis and stabilization of AgNPs.

The TEM images were captured at magnifications of 94000 X to 630 KX, as shown in (Figs. 4A-4C). TEM images clearly revealed the spherical and quasi-spherical shapes of the AgNPs, demonstrating their uniform dispersion and separation without any agglomeration. The particles maintained indirect contact due to the protein capping agent. The crystalline nature of the AgNPs was definitively confirmed by analyzing SAED pattern (Fig. 4D), which exhibited a well-defined diffraction lattice in the silver region, thus confirming the crystalline structure of the synthesized particles **[13]**.

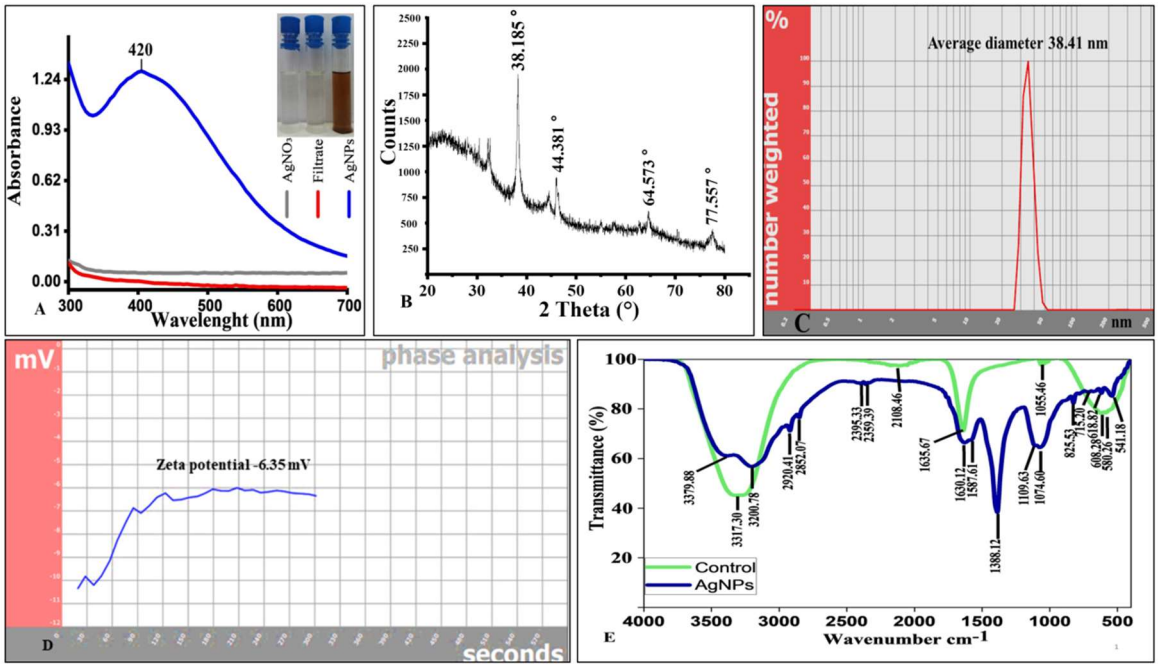

Figure 3. Characterization of the biosynthesized AgNPs: **A**. UV-visible absorption spectra. **B**. XRD Pattern. **C**. DLS measurements. **D**. Zeta potential analysis. **E**. FTIR analysis

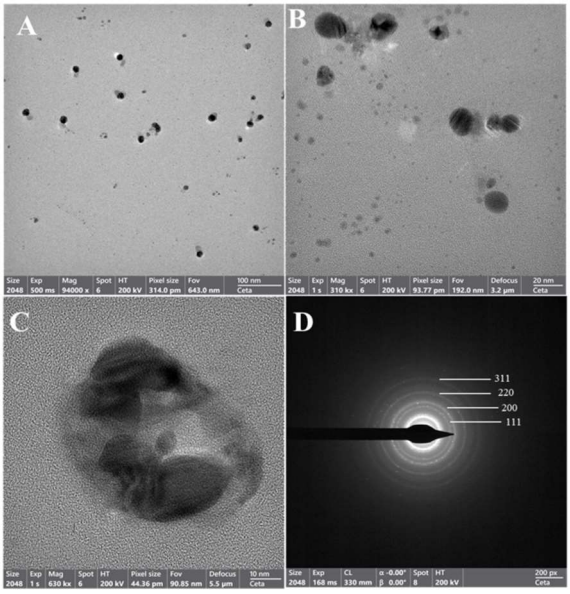

Figure 4. TEM images of AgNPs: **A**, **B**, **C**. Nanoparticles images at different scale bars. **D**. SAED pattern.

3.3. Optimization of AgNPs biosynthesis

Mycosynthesis of AgNPs with varying concentrations of $AgNO_3$ solution from 0.1 to 5 mM was investigated (Fig. 5). The results indicated that 1 mM concentration significantly enhanced the consistent synthesis of AgNPs. The production of AgNPs increased as the $AgNO_3$ concentration increased from 0.1 to 1.0 mM and then started to decrease. An increase in $AgNO_3$ concentration resulted in larger particle size and aggregation of the biosynthesized AgNPs [22].

The extracellular biosynthesis of AgNPs was observed using varying amounts of fungal biomass (5, 10, 15 and 20 g). The recorded UV–visible absorption spectra at 420 nm are shown in (Fig. 5). The optimal wet weight of fungal biomass was determined to be 5 g, as the production of AgNPs decreased with an increase in biomass weight. The concentration of the reducing agent in the green synthesis of nanoparticles was shown to be crucial in controlling the yield of formation, size, and shape of nanoparticles [61].

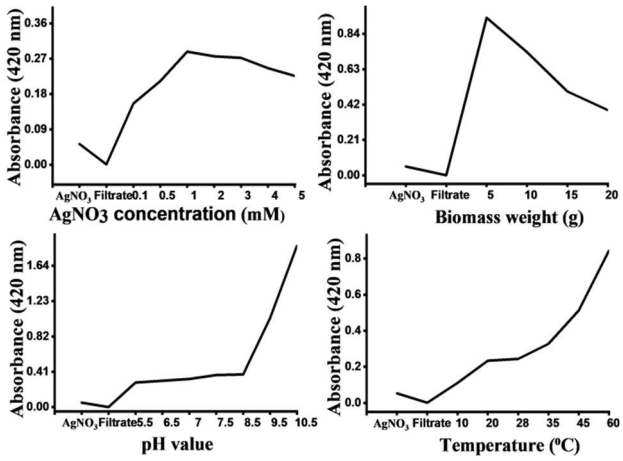

Figure 5. The effect of different reaction parameters on AgNPs biosynthesis.

In this study, the influence of pH on the biosynthesis of AgNPs was examined. Different pH values ranging from 5.5 to 10.5 were tested and revealed that the biosynthesis of AgNPs was most significant at pH 10.5 (Fig. 5). The enzyme and protein produced demonstrated greater reducing and stabilizing capabilities in an alkaline environment than in acidic mixtures [62]. The obtained results indicated that *C. spicifera* has a strong capacity for biosynthesizing AgNPs, with maximum absorbance peaks observed at pH value of 10.5.

The impact of temperature in the biosynthesis processis was investigated by incubating the reaction mixture at different temperatures and recording the UV-visible absorption spectra at 420 nm, as shown in (Fig. 5). The findings indicated that higher reaction temperatures promote the biosynthesis of AgNPs. The temperature used in the synthesis of AgNPs with fungi can affect various parameters such as synthesis speed, size and stability of the AgNPs [63]. According to the results, the optimal temperature for AgNPs biosynthesis by *C. spicifera* was found to be 60°C.

3.4. Evaluation of the antimicrobial activity of the biosynthesized AgNPs

The efficacy of AgNPs as an antimicrobial agent was assessed against pathogenic bacteria and yeast strains (Table 1, Fig. 6). At a concentration of 50 µg, AgNPs demonstrated significant efficacy against Gram-negative bacteria, particularly *E. coli*, with an observed inhibition zone diameter of 23.7±0.3 mm. The effect on *P. aeruginosa* at the same concentration was of around 15.7±0.3 mm. The results indicated a pronounced effect on Gram-positive bacteria, indicating the the broad-spectrum antimicrobial effect of AgNPs. Among the yeast strains, *C. albicans* showed the highest susceptibility to AgNPs at 50 µg, with an inhibition zone diameter of 16.7±0.1 mm. The results indicated a consistent increase in the inhibition zone with increasing AgNPs concentration. The results are align with those of Li et al. [64] who reported inhibition zone diameters of 16.0±1.0 mm for *C. albicans*, 14±1.0 mm for *C. tropicalis*, 13.0±1.0 mm for *E. coli*, 12.0±1.0 mm for *P. aeruginosa* and 16.0±1.0 mm for *S. aureus* at 20 µg of AgNPs biosynthesized by *Aspergillus terreus*. AgNPs from *Ocimum tenuiflorum* showed inhibition zone diameter of 24.1±0.31, 22.3±0.29 and 21.5±0.42 mm against *E. coli*, *P. aeruginosa* and *S. aureus*, respectively [65]. Biogenic AgNPs from *Aspergillus brunneoviolaceus* exhibited inhibition zone diameter of 17.0±0.29, 19.0±0.31 and 19.0±0.32 mm against *E. coli*, *P. aeruginosa* and *S. aureus*, respectively [13]. AgNPs biosynthesized by *Aspergillus hiratsukae* demonstrated inhibition zone diameter of 19.3±1.5, 14.9±1.1 and 12.2±1.4 mm against *E. coli*, *S. aureus*, and *C. albicans*, respectively [18]. Green synthesized AgNPs from previous studies exhibited inhibition zone diameter range 9.5–19.3 mm against *E. coli*, *P. aeruginosa*, *S. aureus* and *C. albicans* [1, 14, 17, 21, 66].

The MICs of AgNPs was determined for the tested microorganisms, as indicated in the Table 1. AgNPs showed

significant efficacy against *E. coli* and *C. albicans*, with MIC values of 4.2±0.1 µg and 5.7±0.3 µg, respectively. In contrast, *P. aeruginosa* and *G. candidum* exhibited the lowest susceptibility, with MIC values of 6.8±0.1 and 11.3±0.3 µg, respectively. In previous studies the MIC of biosynthesized AgNPs against *E. coli*, *P. aeruginosa*, *B. cereus*, *S. aureus* and *C. albicans* were found to be in range 0.235–7.8 µg/ml [2, 58, 67, 68, 69].

Table 1. Antimicrobial activity and the MIC of AgNPs against pathogenic bacteria and yeast species (P<0.05).

Microorganisms		Inhibition zone diameter in mm								MIC (µg)
		Amp / Flu		Fungal filtrate	$AgNO_3$ (10 µg)	AgNPs (µg)				
						5	10	25	50	
Gram-negative bacteria	*E. coli*	8.3±0.3	Amp: Ampicillin (10 µg)	-	-	12.8±0.1	15.7±0.3	18.5±0.25	23.7±0.3	4.2±0.1
	P. aeruginosa	9.7±0.3		-	-	-	7.3±0.3	12.3±0.3	15.7±0.3	6.8±0.1
Gram-positive bacteria	*B. cereus*	14.3±0.3		-	-	12.7±0.1	16.3±0.3	18.2±0.1	22.5±0.25	4.3±0.1
	S. aureus	13.3±0.1		-	-	12.8±0.1	14.8±0.1	17.3±0.1	21.7±0.3	4.7±0.1
Yeast species	*C. albicans*	7.3±0.3	Flu: Fluconazole (25 µg)	-	-	-	8.5±0.25	13.5±0.25	16.7±0.1	5.7±0.3
	C. tropicalis	11.7±0.3		-	-	-	8.3±0.3	12.5±0.25	15.8±0.1	6.7±0.3
	G. candidum	-		-	-	-	-	11.7±0.3	15.2±0.1	11.3±0.3

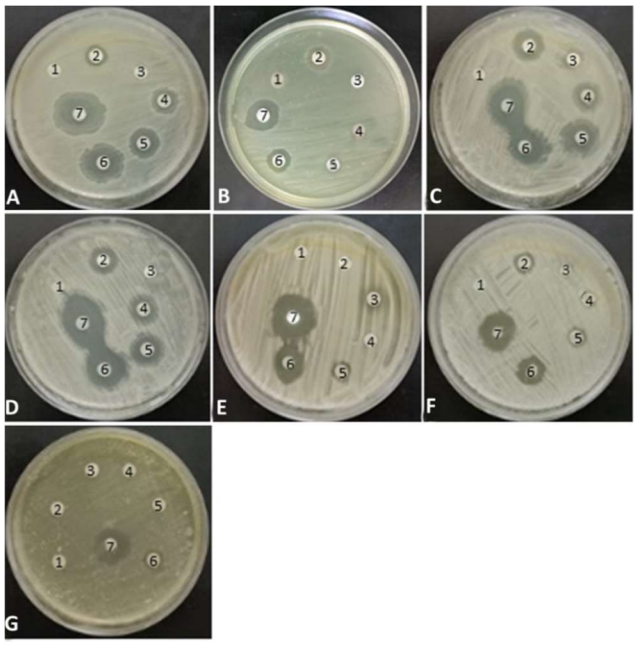

Figure 6. The antimicrobial effect of AgNPs: **A.** *E. coli*. **B.** *P. aeruginosa*. **C.** *B. cereus*. **D.** *S. aureus*. **E.** *C. albicans*. **F.** *C. tropicalis*. **G.** *G. candidum*. **1**. Fungal filtrate. **2**. Ampicillin (10 µg) for A, B, C, D / Fluconazole (25 µg) For E, F, G. **3**. $AgNO_3$. **4**. AgNPs (5 µg). **5**. AgNPs (10 µg). **6**. AgNPs (25 µg). **7**. AgNPs (50 µg).

The MICs of AgNPs bisynthesized by *Aspergillus caespitosus* against *E. coli*, *P. aeruginosa*, *B. cereus*, *S. aureus*, and *C. albicans* were found to be 1.174, 0.235, 0.939, 0.880, and 1.174 mg/ml, respectively [63]. AgNPs biogenic from *Gloeophyllum striatum* were experted MIC values of 15 µM for *E. coli* and *P. aeruginosa*, and 30 µM for *S. aureus* [20]. The MIC of AgNPs against *E. coli*, *S. aureus*, and *C. albicans* were found to be in range 40–500 µg/ml [70, 71].

The AgNPs demonstrated effective antibacterial activity against both Gram-negative and Gram-positive bacteria. However, they exhibited greater antibacterial activity against Gram-negative bacteria than Gram-positive ones. This discrepancy is attributed to the variances in the cell wall structures of the two types of bacteria [5, 21, 72]. AgNPs disrupt the integrity of the bacterial cell wall, which facilitates the permeation of substances into and out of the bacterial cell. This mode of action of AgNPs may also involve the generation of reactive oxygen species, leading to heightened toxicity and the inhibition of the bacteria's respiratory chain [73]. The antimicrobial activity of AgNPs is due to their large surface area and small size, they can adhere to the cell membrane surface, disrupting permeability and respiratory processes, inhibiting enzyme functions, and inactivating DNA replication of bacterial and fungal pathogens [57, 74].

4. Conclusion

In the current study, it was observed that *Curvularia spicifera* (SUMCC 22003), an endophytic fungus isolated from leaves of the medicinal plant *Calotropis procera*, demonstrated significant potential for AgNPs production. The synthesized AgNPs were characterized using UV-visible spectroscopy, revealing a distinct SPR peak at 420 nm. The AgNPs were found to be stable, well-dispersed and spherical, with an average diameter of 38.41 nm and a zeta potential of -6.35 mV. Analysis using XRD and TEM confirmed the crystalline nature of the AgNPs, while FTIR indicated the presence of a capping protein contributing to their stability. The optimized reaction conditions, including 1 mM $AgNO_3$, 5 g of biomass weight, pH 10.5 and a reaction temperature of 60°C, were identified as the ideal biosynthesis model. Furthermore, the biosynthesized AgNPs exhibited potent antimicrobial activity against a range of microorganisms, showcasing their potential as broad-spectrum antimicrobial agents.

CRediT authorship contribution statement
Conceptualization, B.A.E., and M.S.B.; methodology, G.G.F., and M.S.B.; data collection: B.A.E., M.S.B., and G.G.F.; Data curation: B.A.E., M.S.B., and G.G.F.; draft manuscript preparation G.G.F.; review and editing B.A.E., and M.S.B; Project administration B.A.E. All authors have read and agreed to the published version of the manuscript.

Data availability statement
All data generated or analyzed during this study are included in this published article.

Declaration of competing interest
The authors declare no competing interests.

References

[1] P-J. Li, J-J. Pan, L-J. Tao, X. Li, D-L. Su, Y. Shan, et al., *Molecules*, 26 (2021) 4479.
[2] E. I. Murillo-Rábago, A. R. Vilchis-Nestor, K. Juarez-Moreno, L. E. Garcia-Marin, K. Quester, et al., *Antibiotics*, 11 (2022) 800.
[3] J. K. Patra, K-H. Baek, *Frontiers in Microbiology*, 8 (2017) 167.
[4] S. N. H. Azmi, B. M. H. Al-Jassasi, H. M. S. Al-Sawaf, S. H. G. Al-Shukaili, N. Rahman, et al., *Environmental Monitoring and Assessment*, 193 (2021) 497.
[5] N. Al-Gburi, A. Al-Hassnawi, L. A. Al-Bayati, *Medical Journal of Babylon*, 21 (2024) 493-499.
[6] T. P. Devi, S. Kulanthaivel, D. Kamil, J. L. Borah, N. Prabhakaran, et al., *Indian Journal of Experimental Biology*, 51 (2013) 543-547.
[7] I. Ghiuta, C. Croitoru, J. Kost, R. Wenkert, D. Munteanu, (2021). *Applied Sciences*, 11 (2021) 3134.
[8] P. Soleimani, A. Mehrvar, J. P. Michaud, N. Vaez, *Journal of Invertebrate Pathology*, 190 (2022) 107749.
[9] K. Zomorodian, S. Pourshahid, A. Sadatsharifi, P. Mehryar, K. Pakshir, et al., *BioMed research international*, 16 (2016) 5435397.
[10] A. Gul, Fozia, A. Shaheen, I. Ahmed, B. Khattak, et al., *Biomolecules*, 11 (2021) 206.
[11] D. Patel, B. Patel, V. K. Yadav, M. P. Sudhakar, S. A. Alharbi, et al., *Journal of Hazardous Materials Advances*, 16 (2024) 100478.
[12] N. S. Shaligram, M. Bule, R. Bhambure, R. S. Singhal, S. K. Singh, et al., *Process biochemistry*, 44 (2009) 939-943.
[13] H. Mistry, R. Thakor, C. Patil, J Trivedi, H. Bariya, *Biotechnology Letters*, 43 (2021) 307-316.
[14] O. Gemishev, M. Panayotova, G. Gicheva, N. Mintcheva, *Materials*, 15 (2022) 481.
[15] A. Jebali, F. Ramezani, B. Kazemi, *Journal of Cluster Science*, 22 (2011) 225-232.
[16] A. Dhaka, S. C. Mali, S. Sharma, R. Trivedi, *Results in Chemistry*, 6 (2023) 101108.
[17] X. Hu, K. Saravanakumar, T. Jin, M. H. Wang, *International journal of nanomedicine*, 14 (2019) 3427-3438.
[18] E. Saied, M. A. Abdel-Maksoud, A. A. Alfuraydi, B. H. Kiani, M. Bassyouni, et al., *Frontiers in Microbiology*, 15 (2024) 1345423.
[19] K. S. Siddiqi, A. Husen, R. A. K. Rao, *Journal of nanobiotechnology*, 16 (2018) 14.
[20] K. Zawadzka, A. Felczak, M. Nowak, A. Kowalczyk, I. Piwonski, et al., *Journal of Hazardous Materials*, 418 (2021) 126316.
[21] S. Kaviyaa, J. Santhanalakshmi, B. Viswanathan, J. Muthumary, K. Srinivasan, *Spectrochimica Acta Part A*, 79 (2011) 594-598.
[22] N. A. El-Zawawy, A. M. Abou-Zeid, D. M. Beltagy, N. H. Hantera, H. S. Nouh, *Microbial Cell Factories*, 22 (2023) 228.
[23] M. Singhal, L. Loveleen, R. Manchanda, A. Syed, A. H. Bahkali, et al., *Journal of Agriculture and Food Research*, 16 (2024) 101088.
[24] L. R. Jaidev, G. Narasimha, *Colloids and Surfaces B: Biointerfaces,* 81 (2010) 430-433.
[25] M. Govindappa, M. L. avanya, P. Aishwarya, P. Kavya, L. Prathiksha, et al., *BioNanoScience*, 10 (2020) 928-941.
[26] I. Solís-Sandí, S. Cordero-Fuentes, R. Pereira-Reyes, J. R. Vega-Baudrit, D. Batista-Menezes, et al., *Biotechnology Reports*, 40 (2023) e00816.
[27] S. Marutyan, H. Karapetyan, L. Khachatryan, A. Muradyan, S. Marutyan, et al., *Scientifc Reports*, 14 (2024) 19163.
[28] M. Mahdieha, A. Zolanvari, A.S. Azimee, M. Mahdieh, *Scientia Iranica F,* 19 (2012) 926-929.
[29] M. J. Firdhouse, P. Lalitha, *Journal of Nanotechnology,* 5 (2015) 829526.
[30] R. Thiurunavukkarau, S. Shanmugam, K. Subramanian, P. Pandi, G. Muralitharan, et al., *Scientific Reports*, 12 (2022) 14757.
[31] T. L. Nascimento, Y. Oki, D. M. M. Lima, J. S. Almeida-Cortez, G. W. Fernades, et al., *Fungal Ecology*, 14 (2015) 79-86.
[32] H. Batol, M. Hussain, M. Hameed, R. Ahmad, *Big Data in Agriculture (BDA)*, 2 (2020) 29-31.
[33] R. Rani, D. Sharma, M. Chaturvedi, J. P. Yadav, *Clinical Microbiology*, 6 (2017) 280.
[34] W. L. Cui, X. Q. Lu, J. Y. Bian, X. L. Qi, D. W. Li, et al., *Plant Pathology*, 96 (2020) 1139-1147.
[35] S. J. Jeon, T. T. T. Nguyen, H. B. Lee, *Mycobiology*, 43 (2015) 210-217.
[36] J. Hallmann, G. Berg, B. Schulz, Isolation procedures for endophytic microlorganisms. *New York: Springer Brelin Heidelberg*. pp. 299-319, 2007.
[37] M. S. Bakhit, A. E. Abdel-Aziz, Phytotaxa, 511 (2021) 289-295.
[38] T. J. White, T. D. Bruns, S. B. Lee, J.W. Taylor, (1990): Amplification and direct sequencing of fungal ribosomal RNA genes for phylogenetics. In: M. A. Innis, D. Gelfand, J. Sninsky, T. White, (eds). PCR protocol: a guide to methods and applications, *San Diego. CA. Academic Press*, pp. 315-321, 1990.
[39] M. A. Abdel-Wahab, T. Nagahama, Abdel-Aziz F. A. *Mycoscience*, 50 (2009) 147-155.
[40] J. D. Thompson, T. J. Gibson, F. Plewniak, F. Jeanmougin, D. G. Higgins, *Nucleic Acids Research*, 25 (1997) 4876–4882.

[41] D. Edler, J. Klein, A. Antonelli, D. Silvestro, *Methods in Ecology and Evolution*, 12 (2021) 373-377.
[42] A. E. Abdel-Aziz, M. S. Bakhit, *Plant Fungal Syst*. 68 (2023) 232-238.
[43] M. F. Alves, P. G. Murray, *Journal of Fungi*, 8 (2022) 439.
[44] M. Madakka, N. Jayarajub, N. Rajesh, *MethodsX*, 5 (2018) 20-29.
[45] M. liang, S. Wei, L. Jian-Xin, Z. Xiao-Xi, H. Zhi, et al., *Materials Science and Engineering C*, 77 (2017) 963-971.
[46] B. El-Deeb, N. Y. Mostafa, A. Altalhi, Y. Gherbawy, *International Journal of Chemical Engineering*, 30 (2013) 1137-1144.
[47] R. M. Humphries, S. Kircher, A. Ferrell, K. M. Krause, R. Malherbe, et al., *Journal of Clinical Microbiology*, 56 (2018) e00437-18.
[48] A. Veiga, M. G. T. Toledo, L. S. Rossa, M. Mengarda, N. C. F. Stofella, *Journal of Microbiological Methods*, 162 (2019) 50-61.
[49] XLSTAT version 2023.2.0 [Software], Addinsoft. https://www.xlstat.com/en.
[50] K. B. Boedijn, *Bull Jard Bot Buitenzorg*, 13 (1933) 120-134.
[51] M. Arzanlou, S. Khodaei, *Plant Pathology & Quarantine,* 2 (2012) 64-68.
[52] D. S. Manamgoda, L. Cai, E. H. C. McKenzie, P. W. Crous, H. Madrid, et al., *Fungal Diversity*, 56 (2012) 131-144.
[53] B. S. Amaradasa, H. Madrid, J. Z. Groenewald, P. W. Crous, K. Amundsen, *Mycologia*, 106 (2014) 77-85.
[54] T. Sarkar, P. Chakraborty, S. Das, D. Saha, A. Saha, *Canadian Journal of Plant Pathology*, 40 (2018) 594-600.
[55] S. Qostal, S. Kribel, M. Chliyeh, K. Selmaoui, A. O. Touhami, et al., *Plant Cell Biotechnology and Molecular Biology*, 20 (2019) 354-365.
[56] C. Eken, M. Mutlucan, S. Önder, M. Tonguc, S. Erbas, *Notulae Scientia Biologicae*, 16 (2024) 11966.
[57] M. A. Basheer, K. Abutaleb, N. N. Abed, A. A. I. Mekawey, *Journal of Genetic Engineering and Biotechnology*, 21 (2023) 127.
[58] W. A. Lotfy, B. M. Alkersh, S. A. Sabry, H. A. Ghozlan, *Frontiers in Bioengineering and Biotechnology*, 9 (2021) 633468.
[59] M. M. Ramos, E. S. Morais, I. S. Sena, A. L. Lima, F. R. Oliveira, C. M. Freitas, et al., *Biotechnology Letters*, 42 (2020) 833-843.
[60] R. Singh, C. Hano, G. Nath, B. Sharma, *Biomolecules*, 11 (2021) 299.
[61] M. Al-Limoun, H. N. Qaralleh, K. M. Khleifat, M. Al-Anber, A. Al-Tarawneh, *Current Nanoscience*, 15 (2019) 1-13.
[62] M. Othman, M. A. Elsayed, N. G. Al-Balakocy, M. M. Hassan, A. M. Elshafei, et al., *Journal of Genetic Engineering and Biotechnology*, 17 (2019) 8.
[63] M. A. El-Bendary, M. E. Moharam, S. R. Hamed, S. M. Abo El-Ola, S. K. H. Khalil, et al., *Applied Organometallic Chemistry*, 35 (2021) e6338.
[64] G. Li, D. He, Y. Qian, B. Guan, S. Gao, et al., *International Journal of Molecular Sciences*, 13 (2012) 466-476.
[65] H. Bagur, C. C. Poojari, G. Melappa, R. Rangappa, N. Chandrasekhar, et al., *Journal of Cluster Science*, 31 (2020) 1241-1255.
[66] K. Anandalakshmi, J. Venugobal, V. Ramasamy, *Applied in Nanoscience*, 6 (2016) 399-408.
[67] Y. Y. Loo, Y. Rukayadi, M-A-R. Nor-Khaizura, C. H. Kuan, B. W. Chieng, et al., *Frontiers in Microbiology*, 9 (2018) 1555.
[68] S. Tyagi, P. K. Tyagi, D. Gola, N. Chauhan, R. K. Bharti, *SN Applied Sciences*, 1 (2019) 1545.
[69] A. Sharma, A. Sagar, J. Rana, R. Rani, *Micro and Nano Systems Letters*, 10 (2022) 2.
[70] T. Kalaiyarasu, N. Karthi, V. S.Gwri, V. Manju, *Asian Journal Pharmaceutical Clinical Research*, 9 (2016) 1-6.
[71] R. Varghese, M. A. Almalki, S. Ilavenil, J. Rebecca, K. C. Choi, *Saudi Journal of Biological Sciences*, 26 (2019) 148-154.
[72] T. C. Dakal, A. Kumar, R. S. Majumdar, V. Yadav, *Frontiers in Microbiology*, 7 (2016) 1831.
[73] K. M. Khleifat, H. Qaralleh, M. A. Al-kafaween, M. O. Al-limoun, M. Alqaraleh, et al., *Applied Environmental Biotechnology*, 6 (2021) 42-50.
[74] K. Górka, K. Kubiński, *Applied Sciences*, 14 (2023) 115.